High-Resolution Mapping of Phase-Matching Conditions in Second-Order Nonlinear Crystals

C. Dorrer, I. A. Begishev, S.-W. Bahk, and J. Bromage

Laboratory for Laser Energetics, University of Rochester

Nonlinear crystals are widely used for frequency conversion of lasers and optical parametric amplification. Phase matching between the interacting waves is required for efficient operation.[1] This can generally be achieved by temperature or angle tuning, which both allow precise control the optical index. Such global tuning is sufficient when the interacting beams and the crystal have spatially uniform properties. This is a reasonable assumption for relatively small nonlinear crystals. However, the local crystals properties are impacted by environmental stability during growth, stress within the boule, and impurities in the growth solution. These issues are particularly important for the large-aperture ($\sim 40 \times 40$-cm^2) KDP and partially deuterated KDP (DKDP) that are required to support doubling and tripling of inertial confinement fusion laser systems.[2,3] Variations in axis angle θ and deuteration level X can decrease the frequency-conversion efficiency and uniformity. Large-aperture deuterated KDP crystals will be required for optical parametric chirped-pulse–amplification systems delivering ultrashort optical pulses with peak power well beyond 1 PW (Ref. 4).

While x-ray techniques, optical interferometry, and spectroscopy can be used to spatially resolve the physical characteristics of nonlinear crystals, mapping the local phase-matching conditions is a more-direct approach to performance quantification for an actual laser system. This work demonstrates the high-resolution characterization of local phase-matching conditions for second-harmonic generation of a beam at 1053 nm in several laser crystals, including partially deuterated KDP crystals used for broadband optical parametric amplification of pulses at 920 nm by a pump pulse at 526.5 nm (Ref. 5).

A test bed capable of characterizing crystals over apertures as large as 50×50 mm^2 has been developed [Fig. 1(a)]. A Nd:YLF regenerative amplifier seeded by a fiber front end delivers 1053-nm (λ_1) 350-ps pulses collimated to an ~1-mm diameter. The crystal under test (length L) is mounted on two translation stages that provide transverse scanning in front of the static laser beam. The phase-mismatch $\Delta k_{\mathrm{SHG}} L$ for second-harmonic generation (SHG) is proportional to the normalized energy variation $S(x,y) = [\eta(x,y)/(1/2)]-1$, where η is measured at 526.5 nm (λ_2) for the crystal angularly detuned from ideal phase matching [(θ_+) and (θ_-) in Fig. 1(b)]. The nonideal translation stages induce small position-dependent angular rotations of the crystal that can impact phase matching. To alleviate this, the 1053-nm beam is stabilized by a piezo-actuated mirror using the feedback signal from a four-quadrant photodetector on which the beam reflected by the crystal's input face is incident.

As an example of application, the normalized energy variation S is shown in Fig. 2 for a crystal with a deuteration level equal to 98%. For the first two measurements, the input face is the same [labeled as (A) on the figure], whereas the input face is the opposite face for the third measurement [labeled as (B) on the figure]. This crystal has variations in normalized energy up to 25%. Anticorrelated variations of S are obtained when operating at θ_- and θ_+ [Figs. 2(a) and 2(b)]. The high-frequency variations, e.g., in the upper-right corner on Fig. 2(a), are not measurement artifacts. They consistently correspond to a sign change between Figs. 2(a) and 2(b), indicating that they are caused by a local change in phase matching instead of another effect such as low local transmission. This is confirmed by the measured energy variations after a 180° rotation along the vertical axis [Fig. 2(c)]. The low-frequency variations in S are symmetric along the x axis for the two crystal orientations differing by the 180° crystal rotation [Figs. 2(a) and 2(c)]. This indicates that they are caused by bulk variations and do not depend on the propagation direction within the crystal. The observed 25% variations in S are consistent with 20-μrad angular variations and 0.025% deuteration variations.

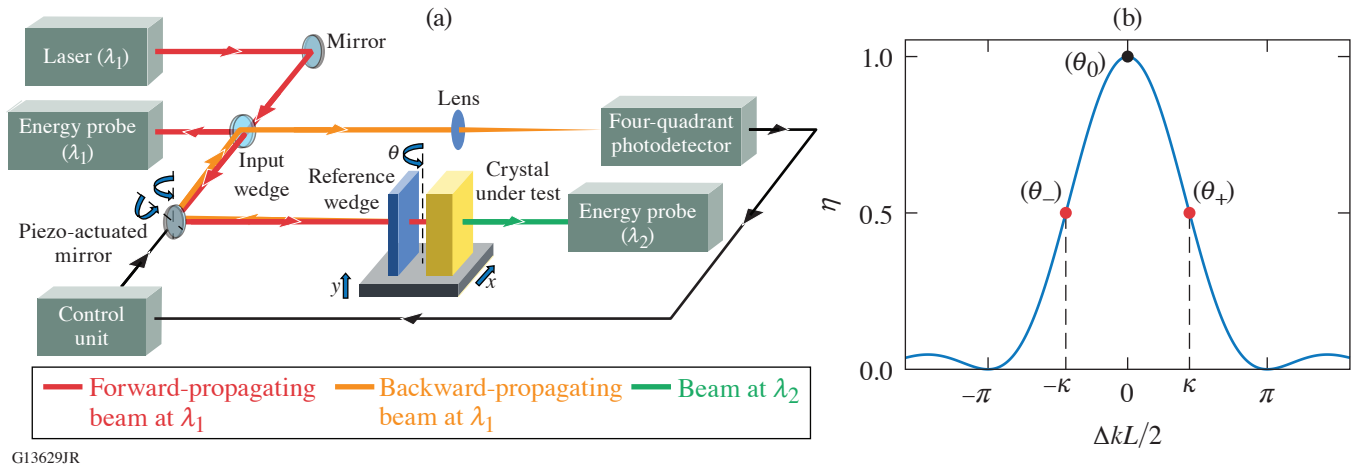

Figure 1
(a) Setup for spatially resolved measurement of the SHG energy, indicating the forward-propagating beam at λ_1 (red line), the backward-propagating beam at λ_1 (orange line), and the beam at λ_2 (green line). (b) Relative SHG efficiency η as a function of the phase mismatch ΔkL.

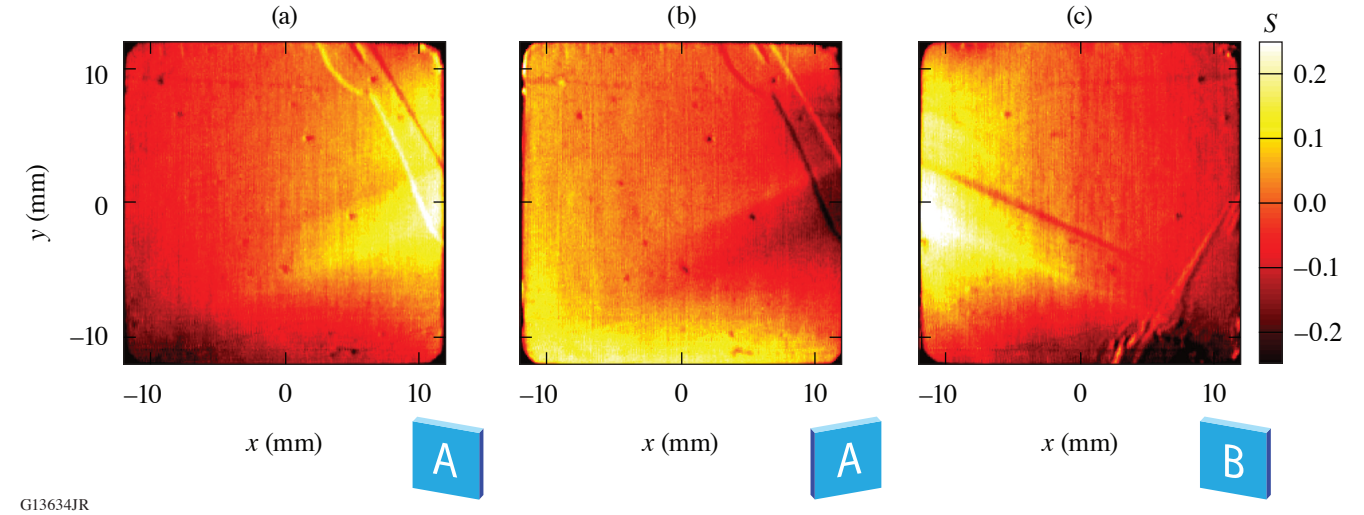

Figure 2
Normalized energy variation S for a crystal with a deuteration level equal to 98%. (a) and (b) correspond to characterization with the same face (A) at the input, and different phase-matching angles θ_- and θ_+, respectively. (c) corresponds to a 180° rotation of the crystal, i.e., characterization with the other face (B) at the input, and phase matching angle θ_-.

The high-frequency variations in S observed in the upper right corner of Fig. 2(a) are, however, not observed in the upper left corner of Fig. 2(c), indicating that these variations are caused by disruptions in phase matching occurring at or close to the input surface. Analytical derivations and experimental results obtained on other crystals confirm that surface variations, such as those introduced by irregularities in sol-gel antireflection coatings, can impact the phase-matching conditions.

A novel approach to the characterization of transverse variations in phase-matching conditions in nonlinear crystals has been demonstrated. SHG in the detuned crystal under test unambiguously converts the local phase mismatch onto energy at the upconverted frequency. Transverse scanning of the crystal combined with beam stabilization maps out phase-matching variations over an aperture only limited by the scanning range of the translation stages. The characterization of partially deuterated

KDP crystals with submillimeter resolution over a 50×50-mm^2 aperture has revealed the impact of spatially nonuniform crystal properties and high-frequency surface variations due to coating imperfections.

The authors thank A. Bolognesi, M. Barczys, T. McKean, and M. Spilatro for experimental assistance with the 1053-nm source. This material is based upon work supported by the Department of Energy National Nuclear Security Administration under Award Number DE-NA0003856, the University of Rochester, and the New York State Energy Research and Development Authority.

1. R. Boyd, *Nonlinear Optics*, 3rd ed. (Academic Press, Amsterdam, 2008), pp. 217–221.
2. J. J. De Yoreo, A. K. Burnham, and P. K. Whitman, Int. Mater. Rev. **47**, 113 (2002).
3. J. M. Auerbach *et al.*, Appl. Opt. **40**, 1404 (2001).
4. C. N. Danson *et al.*, High Power Laser Sci. Eng. **7**, e54 (2019).
5. C. Dorrer *et al.*, Opt. Mater. Express **12**, 3679 (2022).